

Triangular Oxalate Clusters $[W_3(\mu_3-S)(\mu_2-S_2)_3(C_2O_4)_3]^{2-}$ as Building Blocks for Coordination Polymers and Nanosized Complexes

Maxim N. Sokolov,^{*,†} Artem L. Gushchin,[†] Konstantin A. Kovalenko,[†] Eugenia V. Peresyphina,[†] Alexander V. Virovets,[†] Joaquin Sanchiz,[‡] and Vladimir P. Fedin[†]

Nikolaev Institute of Inorganic Chemistry, Siberian Branch of the Russian Academy of Sciences, Lavrentiev Avenue 3, Novosibirsk 630090, Russia, and Departamento de Química Inorgánica, Universidad de La Laguna, 38200 La Laguna, Tenerife, Spain

Received August 15, 2006

The reaction of aqueous $[W_3S_7(C_2O_4)_3]^{2-}$ with Ln^{3+} and Th^{4+} in a 1:1 molar ratio leads to oxalate-bridged heteropolynuclear molecular complexes and coordination polymers. La^{3+} and Ce^{3+} give a layered structure with big (about 1.8 nm) honeycomb pores which are filled with water molecules and lanthanide ions, in $\{[Ln(H_2O)_6]_3[W_3S_7(C_2O_4)_3]_4\}Br \cdot xH_2O$ (**Ia** and **Ib**). The smaller Pr^{3+} , Nd^{3+} , Sm^{3+} , Eu^{3+} , and Gd^{3+} ions give discrete nanomolecules $[(W_3S_7(C_2O_4)_3Ln(H_2O)_5)_2(\mu-C_2O_4)]$ (with a separation of about 3.2 nm between the most distant parts of the molecule), which are further united into zigzag chains by specific $S_2 \cdots Br^-$ contacts to achieve the overall stoichiometry $K[(W_3S_7(C_2O_4)_3Ln(H_2O)_5)_2(\mu-C_2O_4)]Br \cdot xH_2O$ (**Ila–Ild**). Th^{4+} gives $K_2[(W_3S_7(C_2O_4)_3)_4Th_2(OH)_2(H_2O)_{10}] \cdot 14.33H_2O$ (**III**) with a nanosized discrete anion (with a separation of about 2.7 nm between the most distant parts of the molecule), in which two thorium atoms are bound via two hydroxide groups into the $Th_2(OH)_2^{6+}$ unit, and each Th is further coordinated by five water molecules and two monodentate $[W_3S_7(C_2O_4)]^{2-}$ cluster ligands. All compounds were characterized by X-ray structure analysis and IR spectroscopy. Magnetic susceptibility measurements in the temperature range of 2–300 K show weak antiferromagnetic interactions between two lanthanides atoms for compounds **Ila**, **Ilb**, and **Ild**. The thermal decomposition of **Ia**, **Ib**, and **Ild** was studied by thermogravimetry.

Introduction

Coordination polymers based on mononuclear transition metal complexes with multifunctional bridging ligands are attracting much interest because of their potential applications in optoelectronic, magnetic, microporous, and biomimetic materials, as well as of their versatile intriguing architectures and topologies.^{1,2} The design of coordination polymers is highly influenced by diverse factors such as the coordination behavior of metal ions, the structural characteristics of polydentate organic ligands, the metal–ligand ratio, the

possible counterion influence, and last but not the least, non-valence interactions. In some cases, a subtle alteration in any of these factors leads to completely different structures.

In particular, there has been a tremendous activity during the past decade in the area of molecular-based magnets. The oxalate ligand has emerged as a very appealing candidate because of its remarkable ability to mediate electronic effects between paramagnetic metal ions separated by more than 5 Å by adopting the bisbidentate bridging mode.^{1,2,3} Oxophilic Ln^{3+} ions lend themselves especially well to such studies.

In this work we have used the recently prepared cluster oxalate complex $[W_3S_7(ox)_3]^{2-}$ as a building block for the

* To whom correspondence should be addressed. E-mail: caesar@che.nsk.su.

[†] Nikolaev Institute of Inorganic Chemistry, Siberian Branch of the Russian Academy of Sciences.

[‡] Departamento de Química Inorgánica, Universidad de La Laguna.

(1) For selected reviews, see: (a) Eddaoudi, M.; Batten, S. R.; Robson, R. *Angew. Chem., Int. Ed.* **1998**, *37*, 1460. (b) Moler, D. B.; Li, H.; Chen, B.; Reineke, T. M.; O'Keeffe, M.; Yaghi, O. M. *Acc. Chem. Res.* **2001**, *34*, 319. (c) Moulton, B.; Zaworotko, M. J. *Chem. Rev.* **2001**, *101*, 1629. (d) Kim, K. *Chem. Soc. Rev.* **2002**, *31*, 96. (e) Evans, O. R.; Lin, W. *Acc. Chem. Res.* **2002**, *35*, 511. (f) Kitagawa, S.; Noro, S. *Chem. Commun.* **2006**, 701. (g) Kitagawa, S.; Kitaura, R.; Noro, S. *Angew. Chem., Int. Ed.* **2004**, *43*, 2334. (h) Ferey, G.; Mellot-Drazhnieks, C.; Serre, C.; Millage, F. *Acc. Chem. Res.* **2005**, *38*, 217.

(2) (a) Tong, M.-L.; Chen, X.-M.; Ye, B.-H.; Ji, L.-N. *Angew. Chem., Int. Ed.* **1999**, *38*, 2237. (b) Eddaoudi, M.; Li, H.; Yaghi, O. M. *J. Am. Chem. Soc.* **2000**, *122*, 1391. (c) Min, K. S.; Suh, M. P. *J. Am. Chem. Soc.* **2000**, *122*, 6834. (d) Kiang, Y.-H.; Gardner, G. B.; Lee, S.; Xu, Z. *J. Am. Chem. Soc.* **2000**, *122*, 6871. (e) Jung, O.-S.; Kim, Y. J.; Lee, Y.-A.; Park, J. K.; Chae, H. K. *J. Am. Chem. Soc.* **2000**, *122*, 9921. (f) Hong, M.; Zhao, Y.; Su, W.; Cao, R.; Fujita, M.; Zhou, Z.; Chan, A. S. C. *Angew. Chem., Int. Ed.* **2000**, *39*, 2468. (g) Lu, J. Y.; Babb, A. M. *Inorg. Chem.* **2001**, *40*, 3261. (h) Fu, A.; Huang, X.; Li, J. Yuen, T.; Lin, C. L. *Chem.—Eur. J.* **2002**, *8*, 2239.

(3) Kahn, O. *Molecular Magnetism*; VCH: Weinheim, Germany, 1993.

construction of nanosized complexes and coordination polymers with rare earths and Th^{4+} ions. The tungsten atoms in the W_3S_7 cluster core are bidentately coordinated by oxalate ligands and each oxalate ligand has two vacant coordination places available for bridging and making extended structures. The S_2 ligands in the $\text{W}_3\text{S}_7^{4+}$ core participate in specific non-valence interactions and influence the packing to a large extent. The interplay of these two factors creates the interesting structural features presented below.

Experimental Section

Materials and Methods. The starting potassium salt of $[\text{W}_3\text{S}_7(\text{C}_2\text{O}_4)_3]^{2-}$ was prepared as described in the work.⁴ All the other reagents were purchased from commercial sources and used without further purification.

Elemental analyses were carried out by the Novosibirsk Institute of Organic Chemistry microanalytical service. IR spectra (4000–400 cm^{-1}) were recorded on a Scimitar FTS 2000 Fourier spectrometer. Thermogravimetric studies were done in an Ar atmosphere on a Netzsch TG 209 apparatus, at a rate of 10 $^\circ\text{C min}^{-1}$. A Quattro LC (quadrupole–hexapole–quadrupole) mass spectrometer with an orthogonal Z-spray-electrospray interface (Micromass, Manchester, U.K.) was used. The drying gas, as well as the nebulizing gas, was nitrogen at a flow rate of 400 and 80 L h^{-1} , respectively. Sample solutions in methanol were infused via syringe pump directly to the interface at a flow rate of 6 $\mu\text{L min}^{-1}$. A capillary voltage of 3.5 kV was used in the negative scan mode, and the cone voltage was varied between –10 to –60 V. The chemical composition of each peak was assigned by comparison of calculated and observed isotope patterns using the MassLynx 3.5 program.⁵ Magnetic susceptibility measurements on polycrystalline samples were carried out in the temperature range of 2–300 K with a Quantum Design SQUID magnetometer with an applied field of 500 Oe for $T < 15$ K and 5000 Oe for $T > 15$ K. Diamagnetic corrections of the constituent atoms were estimated from Pascal's constants.

Synthesis of $\{[\text{La}(\text{H}_2\text{O})_6]_3[\text{W}_3\text{S}_7(\text{C}_2\text{O}_4)_3]_4\}\text{Br}\cdot 24.35\text{H}_2\text{O}$ (Ia). A solution of $\text{K}_2[\text{W}_3\text{S}_7(\text{C}_2\text{O}_4)_3]\cdot 0.5\text{KBr}\cdot 5\text{H}_2\text{O}$ (50 mg, 0.04 mmol) in 10 mL of H_2O was added to 8 mL of a 0.005 M solution of $\text{La}(\text{NO}_3)_3\cdot 6\text{H}_2\text{O}$ (0.04 mmol). The resultant solution became cloudy after few minutes and was kept in a closed vial at room temperature without filtration. The crystals of the product separated after 2 days. They were removed by decantation and washed with ethanol and ether, and dried in air for 2 days. Yield: 18 mg (32%). Anal. Calcd for $\text{C}_{24}\text{H}_{36}\text{BrLa}_3\text{O}_{66}\text{S}_{28}\text{W}_{12}\cdot 16\text{H}_2\text{O}$: C, 5.47; H, 1.30. Found: C, 5.23; H, 1.09. IR (KBr, 4000–400 cm^{-1}): 3420 s, 1703 s, 1671 s, 1432 w, 1388 m, 1318 vw, 1282 vw, 1246 vw, 913 vw, 800 w, 751 vw, 669 vw, 605 vw, 538 w, 469 vw. DTG: 20–150 $^\circ\text{C}$, $\Delta m = 9.5\%$ (–28 H_2O).

Synthesis of $\{[\text{Ce}(\text{H}_2\text{O})_6]_3[\text{W}_3\text{S}_7(\text{C}_2\text{O}_4)_3]_4\}\text{Br}\cdot 24.95\text{H}_2\text{O}$ (Ib). The synthesis is the same as that described above. A solution of $\text{K}_2[\text{W}_3\text{S}_7(\text{C}_2\text{O}_4)_3]\cdot 0.5\text{KBr}\cdot 5\text{H}_2\text{O}$ (50 mg, 0.04 mmol) in 10 mL of H_2O was added to 8 mL of a 0.005 M solution of $\text{Ce}(\text{NO}_3)_3\cdot 6\text{H}_2\text{O}$ (0.04 mmol). Yield: 23 mg (41%). Anal. Calcd for $\text{C}_{24}\text{H}_{36}\text{BrCe}_3\text{O}_{66}\text{S}_{28}\text{W}_{12}\cdot 10\text{H}_2\text{O}$: C, 5.58; H, 1.09. Found: C, 5.70; H, 0.96. IR (KBr, 4000–400 cm^{-1}): 3438 s, 1702 s, 1662 s, 1437 vw, 1387 m, 1284 vw, 913 vw, 801 w, 602 vw, 539 w, 464 vw. DTG: 20–150 $^\circ\text{C}$, $\Delta m = 10.5\%$ (–31 H_2O).

Synthesis of $\text{K}[(\text{W}_3\text{S}_7(\text{C}_2\text{O}_4)_3\text{Pr}(\text{H}_2\text{O})_5)_2(\mu\text{-C}_2\text{O}_4)]\text{Br}\cdot 14.7\text{H}_2\text{O}$ (IIa). The synthesis is the same as that described above. A solution of $\text{K}_2[\text{W}_3\text{S}_7(\text{C}_2\text{O}_4)_3]\cdot 0.5\text{KBr}\cdot 5\text{H}_2\text{O}$ (80 mg, 0.06 mmol) in 14 mL of H_2O was added dropwise into 2.5 mL of 0.025 M solution of $\text{PrCl}_3\cdot 7\text{H}_2\text{O}$ (0.06 mmol). Yield: 35 mg (40%). Anal. Calcd for $\text{C}_{14}\text{H}_{20}\text{BrO}_{38}\text{KPr}_2\text{S}_{14}\text{W}_6$ (without crystal water molecules): C, 6.12; H, 0.73. Found: C, 5.98; H, 0.62. IR (KBr, 4000–400 cm^{-1}): 3345 s, 1702 s, 1648 s, 1442 w, 1392 m, 1315 vw, 1283 vw, 1223 vw, 912 w, 799 m, 604 vw, 538 m, 482 w.

Synthesis of $\text{K}[(\text{W}_3\text{S}_7(\text{C}_2\text{O}_4)_3\text{Nd}(\text{H}_2\text{O})_5)_2(\mu\text{-C}_2\text{O}_4)]\text{Br}\cdot 14\text{H}_2\text{O}$ (IIb). The synthesis is the same as that described above. A solution of $\text{K}_2[\text{W}_3\text{S}_7(\text{C}_2\text{O}_4)_3]\cdot 0.5\text{KBr}\cdot 5\text{H}_2\text{O}$ (80 mg, 0.06 mmol) in 10 mL of H_2O was added to 2.5 mL of 0.025 M solution of $\text{NdCl}_3\cdot 6\text{H}_2\text{O}$ (0.06 mmol). Yield: 28 mg (64%). Anal. Calcd for $\text{C}_{14}\text{H}_{20}\text{BrNd}_2\text{O}_{38}\text{KS}_{14}\text{W}_6\cdot 6\text{H}_2\text{O}$: C, 5.87; H, 1.13. Found: C, 5.53; H, 0.77. IR (KBr, 4000–400 cm^{-1}): 3389 s, 1701 s, 1660 s, 1439 w, 1385 m, 1320 vw, 1283 vw, 1241 vw, 913 vw, 800 m, 605 vw, 538 m, 459 vw. DTG: 20–170 $^\circ\text{C}$, $\Delta m = 11\%$ (–18 H_2O); 250–390 $^\circ\text{C}$, $\Delta m = 17\%$ (–7 CO_2 , –7 CO). ESI-MS (H_2O): 520 ($[\text{W}_3\text{S}_7(\text{ox})_3]^{2-}$, 504 ($[\text{W}_3\text{S}_6(\text{ox})_3]^{2-}$, 488 ($[\text{W}_3\text{S}_5(\text{ox})_3]^{2-}$, 176–181 ($[\text{Nd}(\text{OH})_2]^{+}$, 193–198 ($[\text{Nd}(\text{H}_2\text{O})(\text{OH})_2]^{+}$).

Synthesis of $\text{K}[(\text{W}_3\text{S}_7(\text{C}_2\text{O}_4)_3\text{Sm}(\text{H}_2\text{O})_5)_2(\mu\text{-C}_2\text{O}_4)]\text{Br}\cdot 13.33\text{H}_2\text{O}$ (IIc). The synthesis is the same as that described above. A solution of $\text{K}_2[\text{W}_3\text{S}_7(\text{C}_2\text{O}_4)_3]\cdot 0.5\text{KBr}\cdot 5\text{H}_2\text{O}$ (50 mg, 0.04 mmol) in 10 mL of H_2O was added to 8 mL of a 0.005 M solution of $\text{Sm}(\text{NO}_3)_3\cdot 6\text{H}_2\text{O}$ (0.04 mmol). Yield: 9 mg (15%). Anal. Calcd for $\text{C}_{14}\text{H}_{20}\text{BrO}_{38}\text{KSm}_2\text{S}_{14}\text{W}_6\cdot 6\text{H}_2\text{O}$: C, 5.85; H, 1.12. Found: C, 5.79; H, 0.98. IR (KBr, 4000–400 cm^{-1}): 3335 s, 1703 s, 1668 s, 1436 m, 1384 m, 1319 vw, 1284 vw, 1224 vw, 913 vw, 803 m, 537 m, 464 w.

Synthesis of $\text{K}[(\text{W}_3\text{S}_7(\text{C}_2\text{O}_4)_3\text{Gd}(\text{H}_2\text{O})_5)_2(\mu\text{-C}_2\text{O}_4)]\text{Br}\cdot 13.17\text{H}_2\text{O}$ (IId). The synthesis is the same as that described above. A solution of $\text{K}_2[\text{W}_3\text{S}_7(\text{C}_2\text{O}_4)_3]\cdot 0.5\text{KBr}\cdot 5\text{H}_2\text{O}$ (162 mg, 0.13 mmol) in 25 mL of H_2O was added to 5 mL of a 0.025 M solution of $\text{GdCl}_3\cdot 6\text{H}_2\text{O}$ (0.13 mmol). Yield: 130 mg (67%). Anal. Calcd for $\text{C}_{14}\text{H}_{20}\text{BrGd}_2\text{O}_{38}\text{KS}_{14}\text{W}_6\cdot 13\text{H}_2\text{O}$: C, 5.58; H, 1.54. Found: C, 5.58; H, 1.54. IR (KBr, 4000–400 cm^{-1}): 3389 s, 1703 s, 1668 s, 1442 m, 1386 s, 1322 vw, 1284 vw, 1242 vw, 1041 vw, 913 vw, 801 m, 636 vw, 606 vw, 539 w, 458 w.

Synthesis of $\text{K}_2[(\text{W}_3\text{S}_7(\text{C}_2\text{O}_4)_3)_4\text{Th}_2(\text{OH})_2(\text{H}_2\text{O})_{10}]\cdot 14.33\text{H}_2\text{O}$ (III). The synthesis is the same as that described above. A solution of $\text{K}_2[\text{W}_3\text{S}_7(\text{C}_2\text{O}_4)_3]\cdot 0.5\text{KBr}\cdot 5\text{H}_2\text{O}$ (50 mg, 0.04 mmol) in 10 mL of H_2O was added to 8 mL of a 0.005 M solution of $\text{ThCl}_4\cdot 8\text{H}_2\text{O}$ (0.04 mmol). Yield: 15 mg (29%). Anal. Calcd for $\text{C}_{24}\text{H}_{22}\text{O}_{60}\text{K}_2\text{S}_{28}\text{Th}_2\text{W}_{12}\cdot 14\text{H}_2\text{O}$: C, 5.58; H, 0.98. Found: C, 5.46; H, 1.14. IR (KBr, 4000–400 cm^{-1}): 3420 s, 2928 w, 1704 s, 1668 s, 1468 vw, 1421 vw, 1373 s, 1272 vw, 1221 vw, 1134 vw, 1041 vw, 911 w, 799 m, 603 vw, 542 m, 482 w.

X-ray Structure Determinations. Crystals of **Ia**, **Ib**, **IIa–IId**, and **III** are orange slates or needles, and all but **III** are extremely unstable in air because of the loss of the water of crystallization. Crystallographic data and structure refinement details are given in Table 1. Diffraction data for all compounds were collected on a Bruker X8APEX CCD diffractometer with Mo $\text{K}\alpha$ radiation ($\lambda = 0.71073$ Å) using ϕ and ω scans of narrow (0.5°) frames. All structures were solved by direct methods and refined by full-matrix least-squares treatment against $|F|^2$ in anisotropic approximation using SHELX97 programs set.⁶ Since **Ia** was found to be isostructural with **Ib** and **IIb–IId** with **IIa**, the same model was used to refine all isostructural compounds. Absorption corrections were

(4) Sokolov, M. N.; Gushchin, A. L.; Naumov, Y. D.; Gerasko, O. A.; Fedin, V. P. *Inorg. Chem.* **2005**, *44*, 2431.

(5) *Masslynx 3.2*; Micromass: Manchester, U.K., 1998.

(6) Sheldrick, G. M. *SHELXS97 and SHELXL97, Programs for the Refinement of Crystal Structures*; Göttingen University: Göttingen, Germany, 1997.

Table 1. Crystallographic Data for I–III^a

	Ia	Ib	IIa	IIb
chemical formula	C ₂₄ H _{84.70} BrLa ₃ O _{90.35} S ₂₈ W ₁₂	C ₂₄ H _{85.90} BrCe ₃ O _{90.95} S ₂₈ W ₁₂	C ₁₄ H _{49.40} BrKO _{52.70} Pr ₂ S ₁₄ W ₆	C ₁₄ H ₄₈ BrKNd ₂ O ₅₂ S ₁₄ W ₆
<i>M_r</i>	5419.74	5434.18	3013.91	3007.95
cell setting	hexagonal	hexagonal	monoclinic	monoclinic
space group	<i>P</i> 32	<i>P</i> 32	<i>C</i> 2/ <i>c</i>	<i>C</i> 2/ <i>c</i>
temp (K)	90.0(2)	90.0(2)	90.0(2)	90.0(2)
<i>a</i> (Å)	25.4465(3)	25.3218(6)	22.0999(6)	21.9015(4)
<i>b</i> , (Å)	25.4465	25.3218	18.6732(5)	18.8307(4)
<i>c</i> , (Å)	13.2492(3)	13.2303(5)	16.4904(6)	16.3162(3)
α (deg)	90	90	90	90
β (deg)	90	90	100.7460(10)	99.2490(10)
γ (deg)	120	120	90	90
<i>V</i> (Å ³)	7429.8(2)	7346.6(4)	6685.9(4)	6641.7(2)
<i>Z</i>	2	2	4	4
<i>D_x</i> (Mg m ⁻³)	2.423	2.457	2.994	3.008
radiation type	Mo Kα	Mo Kα	Mo Kα	Mo Kα
no. of reflns	8430	7363	5433	9105
for cell params				
μ (mm ⁻¹)	10.84	11.02	12.91	13.09
abs correction	empirical (using intensity measurements)	empirical (using intensity measurements)	empirical (using intensity measurements)	empirical (using intensity measurements)
measured reflns	92 265	24 529	19 706	31 045
independent reflns	11 404	11 234	7485	7599
observed reflns	10 813	9801	5373	6119
criterion for observed reflns	<i>I</i> > 2σ(<i>I</i>)	<i>I</i> > 2σ(<i>I</i>)	<i>I</i> > 2σ(<i>I</i>)	<i>I</i> > 2σ(<i>I</i>)
<i>R_{int}</i>	0.048	0.039	0.044	0.041
<i>R</i> [<i>F</i> ² > 2σ(<i>F</i> ²)]	0.025	0.036	0.042	0.036
<i>R_w</i> (<i>F</i> ²)	0.065	0.092	0.100	0.090
<i>S</i>	1.04	0.75	1.02	1.02
no. of reflns	11 404	11 234	7485	7599
no. of params	533	530	416	429
weighting scheme	calcd <i>w</i> = 1/[σ ² (<i>F_o</i> ²) + (0.029 <i>P</i>) ² + 36.4203 <i>P</i>], where <i>P</i> = (<i>F_o</i> ² + 2 <i>F_c</i> ²)/3	calcd <i>w</i> = 1/[σ ² (<i>F_o</i> ²) + (0.0453 <i>P</i>) ² + 179.604 <i>P</i>], where <i>P</i> = (<i>F_o</i> ² + 2 <i>F_c</i> ²)/3	calcd <i>w</i> = 1/[σ ² (<i>F_o</i> ²) + (0.0376 <i>P</i>) ² + 125.3853 <i>P</i>], where <i>P</i> = (<i>F_o</i> ² + 2 <i>F_c</i> ²)/3	calcd <i>w</i> = 1/[σ ² (<i>F_o</i> ²) + (0.0318 <i>P</i>) ² + 293.7753 <i>P</i>], where <i>P</i> = (<i>F_o</i> ² + 2 <i>F_c</i> ²)/3
Flack param	-0.008 (6)	-0.015 (9)		

	IIc	IId	III
chemical formula	C ₁₄ H _{46.66} BrKO _{51.33} S ₁₄ Sm ₂ W ₆	C ₁₄ H _{46.33} BrGd ₂ KO _{51.17} S ₁₄ W ₆	C ₂₄ H ₅₂ K ₂ O _{74.33} S ₂₈ Th ₂ W ₁₂
<i>M_r</i>	3008.10	3018.97	5174.75
cell setting	monoclinic	monoclinic	triclinic
space group	<i>C</i> 2/ <i>c</i>	<i>C</i> 2/ <i>c</i>	<i>P</i> ⁻¹
temp (K)	100.0(2)	90.0(2)	90.0(2)
<i>a</i> (Å)	22.0847(5)	21.7720(6)	14.1102(7)
<i>b</i> , (Å)	18.5430(5)	18.6154(6)	14.2403(6)
<i>c</i> , (Å)	16.5508(4)	16.0027(4)	14.8756(12)
α (deg)	90	90	106.730(3)
β (deg)	100.8530(10)	95.344(2)	102.710(3)
γ (deg)	90	90	109.409(2)
<i>V</i> (Å ³)	6656.6(3)	6457.6(3)	2529.6(3)
<i>Z</i>	4	4	1
<i>D_x</i> (Mg m ⁻³)	3.002	3.105	3.397
radiation type	Mo Kα	Mo Kα	Mo Kα
no. of reflns	6539	5450	3225
for cell params			
μ (mm ⁻¹)	13.27	13.91	17.27
abs correction	empirical (using intensity measurements)	empirical (using intensity measurements)	empirical (using intensity measurements)
measured reflns	29 749	26 721	19 968
independent reflns	7653	7327	11 530
observed reflns	6368	6262	7342
criterion for observed reflns	<i>I</i> > 2σ(<i>I</i>)	<i>I</i> > 2σ(<i>I</i>)	<i>I</i> > 2σ(<i>I</i>)
<i>R_{int}</i>	0.032	0.034	0.054
<i>R</i> [<i>F</i> ² > 2σ(<i>F</i> ²)]	0.028	0.032	0.047
<i>R_w</i> (<i>F</i> ²)	0.074	0.087	0.094
<i>S</i>	1.11	1.04	1.00
no. of reflns	7653	7327	11 530
no. of params	411	435	664
weighting scheme	calcd <i>w</i> = 1/[σ ² (<i>F_o</i> ²) + (0.0289 <i>P</i>) ² + 136.2214 <i>P</i>], where <i>P</i> = (<i>F_o</i> ² + 2 <i>F_c</i> ²)/3	calcd <i>w</i> = 1/[σ ² (<i>F_o</i> ²) + (0.0366 <i>P</i>) ² + 209.5547 <i>P</i>], where <i>P</i> = (<i>F_o</i> ² + 2 <i>F_c</i> ²)/3	calcd <i>w</i> = 1/[σ ² (<i>F_o</i> ²) + (0.0247 <i>P</i>) ²], where <i>P</i> = (<i>F_o</i> ² + 2 <i>F_c</i> ²)/3
Flack param			

^a Computer programs: Apex2, version 1.27 (Bruker, 2005), SHELXS-97 (Sheldrick, 1990), SHELXL-97 (Sheldrick, 1997), and local programs.

applied empirically using the SADABS program.⁷ The crystallographic data were deposited with the Cambridge Structural Database under deposition codes CCDC 605894–605899 for **Ia**,

Ib, and **IIa–IIId**, respectively, and CCDC 606764 for **III**. The site occupancy factors for disordered K⁺ and H₂O were refined and then fixed in the calculated values. The atoms were refined in an isotropic approximation. Intermolecular contacts and packing motifs were analyzed according to refs 8 and 9 with the TOPOS 4.0 Professional program suit for crystallochemical analysis.¹⁰

(7) APEX2, version 1.08; SAINT, version 7.03; SADABS, version 2.11; Bruker Advanced X-ray Solutions, Bruker AXS Inc.: Madison, WI, 2004.

Results and Discussion

Synthesis and Spectroscopy. The triangular cluster complex, $[\text{W}_3\text{S}_7(\text{C}_2\text{O}_4)_3]^{2-}$, reacts with Ln^{3+} ($\text{Ln} = \text{La}, \text{Ce}$) in water in a molar ratio of 1:1 to form coordination polymers $\{[\text{Ln}(\text{H}_2\text{O})_6]_3[\text{W}_3\text{S}_7(\text{C}_2\text{O}_4)_3]_4\}\text{Br}\cdot x\text{H}_2\text{O}$ (**Ia** and **Ib**). Under the same conditions, reactions with smaller Ln^{3+} (from Pr to Gd) ions result in the formation of nanosized discrete molecules $[(\text{W}_3\text{S}_7(\text{C}_2\text{O}_4)_3\text{Ln}(\text{H}_2\text{O})_5)_2(\text{C}_2\text{O}_4)]$, which crystallize as $\text{K}[(\text{W}_3\text{S}_7(\text{C}_2\text{O}_4)_3\text{Ln}(\text{H}_2\text{O})_5)_2(\text{C}_2\text{O}_4)]\text{Br}\cdot x\text{H}_2\text{O}$ (**IIa**–**IIc**). Extra oxalate comes from partial fragmentation of the parent $[\text{W}_3\text{S}_7(\text{C}_2\text{O}_4)_3]^{2-}$ under reaction conditions; this fact also explains the moderate yields of the complexes. The lanthanides in the Tb–Lu range gave only non-crystalline products, and heating the mixture did not improve the situation. Th^{4+} gives $\text{K}_2[(\text{W}_3\text{S}_7(\text{C}_2\text{O}_4)_3)_4\text{Th}_2(\text{OH})_2(\text{H}_2\text{O})_{10}]\cdot 14.33\text{H}_2\text{O}$ (**III**) with a nanosized discrete anion (with the separation of about 2.7 nm between the most distant parts of the molecule), in which two thorium atoms are bridged by two hydroxides into the $\text{Th}_2(\text{OH})_2^{6+}$ unit, and each Th is further coordinated by five water molecules and two monodentate $[\text{W}_3\text{S}_7(\text{C}_2\text{O}_4)_3]^{2-}$ cluster ligands. These results demonstrate that $[\text{W}_3\text{S}_7(\text{C}_2\text{O}_4)_3]^{2-}$ functions as an effective building block for the construction of the oxalato-bridged heteropolynuclear structures incorporating rare-earth and actinide ions. The partial fragmentation of a parent oxalato complex with the formation of the $\text{Ln}_2(\mu\text{-C}_2\text{O}_4)$ was observed before in the reactions of $[\text{Cr}(\text{bpy})(\text{C}_2\text{O}_4)_2]^-$ with Ln^{3+} ($\text{Ln} = \text{La}, \text{Pr}, \text{Gd}$).¹¹ Our attempts to coordinate Er^{3+} or Pr^{3+} to $[\text{Nb}_2(\text{S}_2)_2(\text{C}_2\text{O}_4)_4]^{4-}$ gave only the corresponding Ln oxalates $\text{Ln}_2(\text{C}_2\text{O}_4)_3\cdot x\text{H}_2\text{O}$.¹² Similarly, $[\text{Cr}(\text{C}_2\text{O}_4)_3]^{3-}$ is destroyed (in water).¹³ It is known that Th(IV) undergoes extensive hydrolysis in aqueous solutions.¹⁴ Polymerization of monomeric hydrolyzed Th(IV) species proceeds usually through $\mu\text{-OH}$ bridges.

Magnetic susceptibility measurements in the temperature range of 2–300 K show antiferromagnetic interactions between two lanthanide ions ($d(\text{Ln}\text{--}\text{Ln}) = 6.5\text{--}6.8 \text{ \AA}$) for **IIa**, **IIb**, and **IIc**. The ground state for a Gd(III) ion is $^8\text{S}_{7/2}$ and it is located at some 10^4 cm^{-1} below the first excited-state and is not perturbed by ligand field effects. For such a species, the TIP is expected to be negligible, and the Zeeman factor g_J is expected to be 2.0. Thus, Gd(III) mononuclear species are expected to follow the Curie law with a $\chi_{\text{M}}T$ value of $7.88 \text{ cm}^3 \text{ mol}^{-1} \text{ K}$.¹⁵ The magnetic properties of **IIc** under

the form of the $\chi_{\text{M}}T$ product versus T [χ_{M} being the magnetic susceptibility per two Gd(III) cations] are shown in Figure S1. The value of $\chi_{\text{M}}T$ at room temperature is $15.81 \text{ cm}^3 \text{ mol}^{-1} \text{ K}$, and this value remains almost constant up to 25 K and decreases at lower temperatures, reaching a value of $10.73 \text{ cm}^3 \text{ mol}^{-1} \text{ K}$ at 2 K. Because **IIc** can be seen as a Gd(III) dinuclear entity, the magnetic behavior of Gd is the expected for a weakly antiferromagnetically coupled dinuclear compound. The magnetic properties of **IIc** have been analyzed by means of a simple dimer law deduced from the isotropic spin Hamiltonian $H = -jS_{\text{Gd}(1)}S_{\text{Gd}(2)}$.¹⁶ The best fit parameters are $j = -0.080(1) \text{ cm}^{-1}$, $g = 2.00(1)$, and $R = 5.1 \times 10^{-5}$. The magnetization curve follows the Brillouin function for two isolated Gd(III) ions with $g = 2.0$ and $S = 7$. The antiferromagnetic coupling is the result of the coupling of orbitals of same symmetry,³ and the low value of the coupling constant is one of the features of the 4f trivalent cations, for which the singly occupied orbitals are very efficiently shielded by the fully occupied 5s and the 5p orbitals and have very little interaction with the orbitals of the bridging ligands.

The magnetic properties of **IIb** are shown in Figure S2. The value of $\chi_{\text{M}}T$ at room temperature is $2.95 \text{ cm}^3 \text{ mol}^{-1} \text{ K}$, slightly lower than the expected for the $^4\text{I}_{9/2}$ ground state and monotonically decrease as T is lowered to reach a value of $1.15 \text{ cm}^3 \text{ mol}^{-1} \text{ K}$ at 2 K. This behavior is mainly related to the thermal depopulation of the ligand field energy levels of the multiplet.^{17,18}

A $\chi_{\text{M}}T$ value of $3.2 \text{ cm}^3 \text{ mol}^{-1} \text{ K}$ is expected for **IIa** in which we have two Pr(III) ions in a $^3\text{H}_4$ ground state ($1.60 \text{ cm}^3 \text{ mol}^{-1} \text{ K}$ per Pr(III) ion). Thus the value of $3.1 \text{ cm}^3 \text{ mol}^{-1} \text{ K}$ obtained is as expected (Figure S3). Here again the decrease of the $\chi_{\text{M}}T$ values upon cooling must be caused by the depopulation of the energy levels splitted by the ligand field effect.^{19,20}

The magnetic properties of **IIc** are not affected by the excited states nor by the ligand field effects. For this compound, it has been possible to obtain the coupling constant, which lies in the range of previous studies. However, the magnetic behavior of **IIb** and **IIa** are more complicated. The $\chi_{\text{M}}T$ values obtained experimentally are very close to those expected for the respective ground states, but they do not follow the Curie law upon lowering of the temperature. This behavior could be the result of the occurrence antiferromagnetic coupling or to the thermal depopulation of the energy levels of the multiplet splitted by the ligand field. We think that this latter factor is the most important in the decay of the $\chi_{\text{M}}T$ values upon cooling.

Thermogravimetric study of $\{[\text{La}(\text{H}_2\text{O})_6]_3[\text{W}_3\text{S}_7(\text{C}_2\text{O}_4)_3]_4\}\text{Br}\cdot 24.35\text{H}_2\text{O}$ (**Ia**), $\{[\text{Ce}(\text{H}_2\text{O})_6]_3[\text{W}_3\text{S}_7(\text{C}_2\text{O}_4)_3]_4\}\text{Br}\cdot 24.95\text{H}_2\text{O}$

(8) Peresyphkina, E. V.; Blatov, V. A. *Acta Crystallogr.* **2000**, B56, 1035.

(9) Peresyphkina, E. V.; Blatov, V. A. *Z. Kristallogr.* **2002**, 217, 91.

(10) Blatov, V. A.; Shevchenko, A. P.; Serezhkin, V. N. *J. Appl. Crystallogr.* **2000**, 33, 1193; <http://topos.ssu.samara.ru>.

(11) (a) Zhang, X.; Cui, Y.; Zheng, F.; Huang, J. *Chem. Lett.* **1999**, 1111. (b) Zhang, X.; Guo, G.; Zheng, F.; Zhou, G.; Liu, J.; Ma, H.; Wang, M.; Zeng, H.; Dong, Z.; Huang, J. *Chin. J. Struct. Chem.* **2002**, 21, 477.

(12) Kalinina, I. V.; Gushchin, A. L.; Samsonenko, D. G.; Gerasimenko, A. V.; Sokolov, M. N.; Fedin, V. P. *Acta Crystallogr.* **2003**, E59, 784.

(13) Decurtins, S.; Gross, M.; Schmalle, H. W.; Ferlay, S. *Inorg. Chem.* **1998**, 37, 2443.

(14) Baes, C. F., Jr.; Meyer, N. J.; Roberts, C. E. *Inorg. Chem.* **1965**, 4, 518.

(15) Andruh, M.; Bakalbassis, E.; Kahn, O.; Trombe, J. C.; Porcher, P. *Inorg. Chem.* **1993**, 32, 1616.

(16) Hernández-Molina, M.; Ruiz-Pérez, C.; López, T.; Lloret, F.; Julve, M. *Inorg. Chem.* **2003**, 42, 5456.

(17) Oczko, G.; Legendziewicz, J.; Wickleder, M. S.; Meyer, G. *J. Alloys Compd.* **2002**, 341, 255.

(18) Baggio, R.; Calvo, R.; Garland, M. T.; Peña, O.; Pereg, M.; Rizzi, A. *Inorg. Chem.* **2005**, 44, 8979.

(19) Legendziewicz, J.; Gawryszewska, P.; Cybinska, J.; Oremek, G. *J. Alloys Compd.* **2004**, 380, 389.

(20) Hernández-Molina, M.; Lorenzo-Luis, P. A.; López, T.; Ruiz-Pérez, C.; Lloret, F.; Julve, M. *CrystrEngComm* **2000**, 31, 1.

(**Ib**), and $\text{K}[(\text{W}_3\text{S}_7(\text{C}_2\text{O}_4)_3\text{Nd}(\text{H}_2\text{O})_5)_2(\text{C}_2\text{O}_4)]\text{Br}\cdot 14\text{H}_2\text{O}$ (**III**) shows that after complete removal both of the water of crystallization and the water molecules coordinated to the lanthanide below 150–170 °C, decomposition of the oxalate ligands starts only at 250 °C. Attempts to remove the water of crystallization from **Ib** by heating at 100 °C (in vacuo) cause a loss of crystallinity.

The IR spectra of **Ia**, **Ib**, **IIa–IIc**, and **III** are similar, and each displays two strong bands at 1701–1704 (narrow) and 1648–1671 cm^{-1} (broad), attributable to the $\nu_{\text{as}}(\text{COO}^-)$ and two bands at 1428–1442 and 1373–1392 cm^{-1} for $\nu_{\text{s}}(\text{COO}^-)$. Deconvolution of the broad bands with maxima at 1648 cm^{-1} for **IIa**, 1660 cm^{-1} for **Ib**, and 1668 cm^{-1} for **IIc** gives two new bands centered at 1676 and 1636 cm^{-1} for **IIa**, 1675 and 1635 cm^{-1} for **Ib**, and 1678 and 1637 cm^{-1} for **IIc**. The appearance of several bands both for ν_{as} and ν_{s} is indicative of the presence of a different environment around the oxalate ligands. In the spectra of $\text{K}_2[\text{W}_3\text{S}_7(\text{C}_2\text{O}_4)_3]\cdot 0.5\text{KBr}\cdot 4\text{H}_2\text{O}$, terminal oxalates appear at 1677 cm^{-1} .²¹ On the other side, in $\text{Ln}_2(\mu\text{-C}_2\text{O}_4)_3\cdot x\text{H}_2\text{O}$, where all oxalates are μ_2 -bridging, $\nu_{\text{as}}(\text{COO}^-)$ appears at 1620–1640 cm^{-1} . Thus, tentatively, in **IIa–IIc**, the bands at 1635–1637 cm^{-1} correspond to the $\text{Ln}_2(\mu\text{-C}_2\text{O}_4)$ unit, those at 1675–1678 cm^{-1} correspond to the terminal oxalates, and those at 1701–1704 cm^{-1} correspond to the $\text{W}(\mu\text{-C}_2\text{O}_4)\text{Ln}$ bridges. The decrease of vibration frequency from W to Ln correlates very well with expected decrease in covalence of the M–O bonds.

Structure Description. The complexes with Ln^{3+} , obtained in this work, can be divided into two structural types designated as types **I** and **II**. Type **I** includes coordination polymers $\{[\text{Ln}(\text{H}_2\text{O})_6]_3[\text{W}_3\text{S}_7(\text{C}_2\text{O}_4)_3]_4\}\text{Br}\cdot x\text{H}_2\text{O}$, $x = 24.3$ –(8) and 25.0(8) for $\text{Ln} = \text{La}$ (**Ia**) and Ce (**Ib**), respectively. Smaller Ln^{3+} cations, $\text{Ln} = \text{Pr}$ (**IIa**), Nd (**IIb**), Sm (**IIc**), and Gd (**IIc**) give $\text{K}[(\text{W}_3\text{S}_7(\text{C}_2\text{O}_4)_3\text{Ln}(\text{H}_2\text{O})_5)_2(\text{C}_2\text{O}_4)]\text{Br}\cdot x\text{H}_2\text{O}$, $x = 13(1)$ –15(1) with a discrete, non-polymeric structure (Type **II**). The Eu complex also belongs to this type according to the cell parameter measurements. Type **III** is represented only by $\text{K}_2[(\text{W}_3\text{S}_7(\text{C}_2\text{O}_4)_3)_4\text{Th}_2(\text{OH})_2(\text{H}_2\text{O})_{10}]\cdot 14.33\text{H}_2\text{O}$. Main bond distance ranges for all complexes are given in Table 2.

The La and Ce compounds crystallize in a trigonal crystal system. The structure contains two independent cluster anions $[\text{W}_3\text{S}_7(\text{ox})_3]^{2-}$, one of them is in a general position (Figure 1a), and the other is on a 3-fold axis (Figure 1b). This rather complex structure is in fact built of distinct subunits, designated **A**, **B**, and **C**. The subunit **A** contains alternating cluster anions linked to the cationic moieties $\text{Ln}(\text{H}_2\text{O})_6^{3+}$ ($\text{CN}(\text{Ln}) = 10$, Figure 2, subunit **A**). This linking produces cationic honeycomb layers $\{[\text{Ln}(\text{H}_2\text{O})_6]_3[\text{W}_3\text{S}_7(\text{C}_2\text{O}_4)_3]_2\}_n^{5n+}$ (Figure 3a). The layers involve only 1/3 of the total number of the cluster anions. The remaining 2/3 form subunit **B**, which contains $\text{Ln}(\text{H}_2\text{O})_6^{3+}$ units, coordinated to two cluster anions through three oxygen atoms of two terminal oxalates. The Ln atom is disordered over two positions related by a

(21) Matyukha, V. A. *Oxalates of Rare-Earth Elements and Actinoids* (in Russian); Siberian Branch of the Russian Academy of Sciences: Novosibirsk, Russia, 1998.

Table 2. Some Characteristic Bond Lengths (Å, min–max, av) for **I–III**

	W–W	W–Seq; W–S _{ax}	W–μ ₃ -S	W–O _{6is} ; W–O _{trms} ^a	S–S(S ₂ ²⁻)	Ln, Th–O _{6x}	Ln, Th–O(H ₂ O); Th–O(OH)	S _{ax} ···Br ⁻ ; S _{ax} ···O(C ₂ O ₄) ^b
Ia	2.6954(4)–2.7023(4)	2.481(2)–2.5038(18), 2.493(8); 2.699(3)	2.3741(19)–2.481(2), 2.40(5)	2.081(5)–2.100(5), 2.090(8); 2.118(5)–2.140(5), 2.13(1)	2.046(2)–2.056(2), 2.051(4)	2.439(14)–2.70(3), 2.57(8)	3.376(2)–3.479(2), 3.42(4)	
	2.6917(6)–2.6968(6), 2.694(3)	2.479(3)–2.502(3), 2.489(8); 2.393(3)–2.413(3), 2.405(7)	2.362(3)–2.479(3), 2.40(6)	2.078(7)–2.099(7), 2.088(9); 2.118(8)–2.133(9), 2.128(7)	2.045–2.051(4), 2.051(5)	2.438(11)–2.689(7), 2.42(2)–2.63(5), 2.53(7)	3.361(3)–3.481(3), 3.41(3)	
	2.6977(6)–2.7081(5), 2.703(5)	2.486(3)–2.499(3), 2.495(6); 2.414(4)	2.363(3)–2.365(2), 2.364(1)	2.074(6)–2.086(7), 2.080(6); 2.126(7)–2.156(6), 2.14(2)	2.057(4)–2.061(4), 2.059(2)	2.464(7)–2.524(7), 2.51(2)	3.022(2)–3.235(3), 3.1(1)	
IIb	2.6982(6)–2.7126(6), 2.7047(7)	2.483(2)–2.499(2), 2.493(7); 2.408(2)–2.414(2), 2.412(2)	2.364(2)–2.367(2), 2.366(2)	2.075(6)–2.090(6), 2.084(8); 2.130(6)–2.156(5), 2.14(1)	2.057(4)–2.061(4), 2.059(2)	2.457(7)–2.516(7), 2.50(2)	3.010(2)–3.207(2), 3.1(1)	
	2.7001(4)–2.7106(4), 2.706(5)	2.4857(18)–2.5031(19), 2.485(2)–2.5038(19), 2.414(3)	2.3646(17)–2.3675(17), 2.366(1)	2.081(5)–2.091(5), 2.085(9); 2.128(5)–2.162(5), 2.14(2)	2.056(2)–2.062(2), 2.058(3)	2.413(5)–2.483(5), 2.46(3)	3.040(2)–3.249(2), 3.1(1)	
IIc	2.7032(4)–2.7068(4), 2.706(2)	2.485(2)–2.5038(19), 2.496(6); 2.4134(19)–2.4249(19), 2.418(4)	2.7032(4)–2.7068(4), 2.706(2)	2.089(5)–2.093(5), 2.091(2); 2.132(6)–2.152(5), 2.14(1)	2.054(3)–2.057(3), 2.056(2)	2.417(7)–2.505(7), 2.45(3)	3.026(3)–3.266(3), 3.1(1)	
	2.6932(8)–2.7121(8), 2.702(6)	2.497(3)–2.515(3), 2.391(4)–2.415(4), 2.405(8)	2.368(3)–2.377(3), 2.373(4)	2.073(8)–2.102(9), 2.09(1); 2.101(9)–2.141(5), 2.12(2)	2.043(5)–2.054(5), 2.050(4)	2.445(10)–2.533(9), 2.50(3); 2.349(9)	2.927(9)–3.153(9), 3.01(9) ^b	

^a O_{6is} and O_{trms} are the oxygen atoms that are cis and trans to the μ₃-S position, respectively. ^b The intermolecular contacts S_{ax}···O(C₂O₄)²⁻ are found only in **III**.

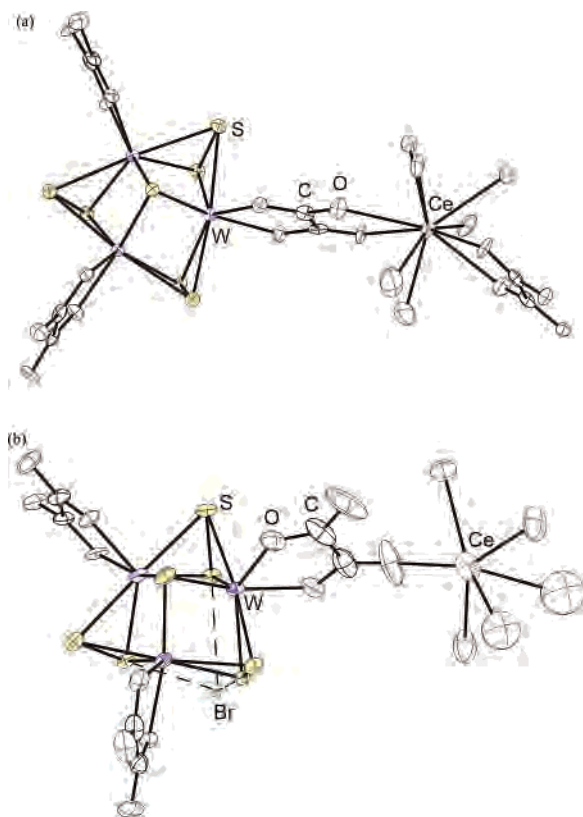


Figure 1. Two independent (a and b) cluster anions and Ln(III) with their coordination environment in **Ib**. W–W bonds are not shown for clarity in this figure and in the following figures; dashed lines show non-valent contacts $S_{ax} \cdots Br$. Ellipsoids are at the 50% probability level (M–M bonds are not shown for clarity).

2-fold axis (space group $P32$, $CN(Ln) = 9$) (Figure 2, subunit **B**). In addition, each cluster anion from **A**, together with three cluster anions from **B**, shares a Br^- anion via short contacts $S_{ax} \cdots Br^-$ (3.38–3.48 Å), to give sandwichlike associates (Figure 2, subunit **C**). The Br^- anion seems to be more strongly attracted to the **A** subunits as follows from the lengths of the corresponding contacts: $S_{ax}(A) \cdots Br^- = 3.36$ – 3.41 Å, $3S_{ax}(B) \cdots Br^- = 3.47$ – 3.48 Å for both **Ia** and **Ib** (Figure 2). It is worth stressing that, although the $S_{ax}-X^-$ contacts are quite common in the structures of M_3S_7 clusters, in most cases they lead to the “true” sandwiches of the type $\{(M_3Q_7)_2X\}$ ($M = Mo, W; Q = S, Se, Te$).^{22–25} Although examples of the $\{W_3S_7\}^{4+}$ clusters are rather scarce in general, $\{(W_3S_7)_2Br\}$ “sandwiches” were observed in $K_{2.5}[W_3S_7(ox)_3]Br_{0.5} \cdot 5H_2O$.⁴ The axial contacts $S_{ax} \cdots Br$ in that case are shorter, 3.100–3.302 Å. The only example of the association of four cluster units around a halide so far known was furnished by $[Mo_3S_7\{(EtO)_2PS_2\}_3]_4I(HgI_3)_3 \cdot 4H_2O$ where $\{(Mo_3S_7)_4I\}$ associates were observed.²⁶ Remarkably, the $S_{ax} \cdots \Gamma$ contacts in the latter are

- (22) Liao, H.; Kanatzidis, M. G. *Inorg. Chem.* **1992**, *31*, 431.
 (23) Virovets, A. V.; Gushchin, A. L.; Abramov, P. A.; Alferova, N. I.; Sokolov, M. N.; Fedin, V. P. *Russ. J. Struct. Chem.* **2006**, *47*, 340.
 (24) Virovets, A. V.; Podberezskaya, N. V. *J. Struct. Chem.* **1993**, *34*, 306.
 (25) Mayor-Lopez, M.; Weber, M.; Hegetschweiler, K.; Meyenberger, M. D.; Jobo, F.; Leoni, S.; Nesper, R.; Reiss, G. J.; Frank, W.; Kolesov, B.; Fedin, V.; Fedorov, V. *Inorg. Chem.* **1998**, *37*, 2633.
 (26) Chen, J.; Lu, S.; Huang, Z.; Yu, R.; Wu, Q. *Chem.—Eur. J.* **2001**, *7*, 2002.

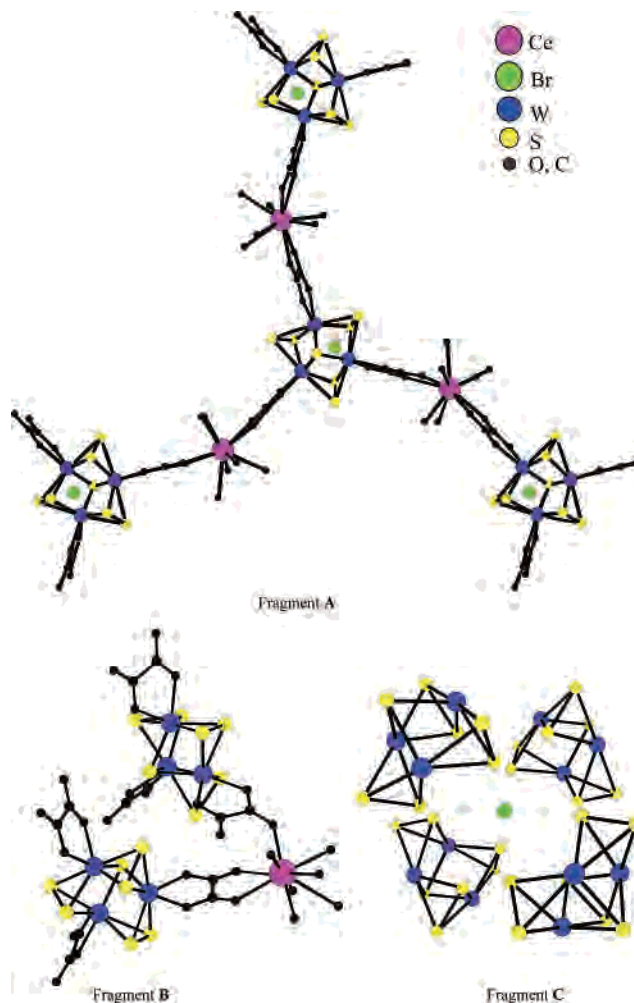


Figure 2. Structural fragments in structure **Ia**: fragment **A** is a structural unit of the layer, fragment **B** is one of two symmetrically disordered positions of Ce(III), coordinated to two clusters through three oxygen atoms of a pair of $C_2O_4^{2-}$ anions, and fragment **C** is composed of four cluster anions forming an agglomerate via axial $S \cdots Br_{ax}$ non-valent contacts. Fragment **C** connects fragments **A** and **B** to form a layer in **I**.

much shorter than in **Ia** and **Ib**, despite I^- being 0.15 Å larger than Br^- . In addition, unlike in **I**, all 12, $S_{ax} \cdots \Gamma$ contacts are related by symmetry and have identical lengths of 3.059 Å. A comparison of the $S_{ax} \cdots Br^-$ contacts in **I** and $K_{2.5}[W_3S_7(ox)_3]Br_{0.5} \cdot 5H_2O$ shows that spatial requirements alone are unlikely to cause such a significant lengthening of the contacts in **I**.

As a whole, structure type **I** can be described as covalent layers, decorated by turns below and above each layer with the sandwich associates (Figure 4). This structure presents the first example of the involvement of a $S_{ax}-X^-$ contact into a polymeric framework. It also features channels which are approximately trigonal in cross-section of about $d_{min} \approx 9.3$ Å in diameter, filled with severely disordered water molecules, in accordance with the hydration number of ~ 25 H_2O per formula unit.

Type **II** structures consists of neutral molecules $[(W_3S_7(ox)_3-Ln(H_2O)_5)_2(ox)]$, $Ln = Pr, Nd, Sm, \text{ and } Gd$ ($CN(Ln) = 9$, Figure 5). Note that apart from these structures, the only molecular structure with the $Ln_2(\mu-C_2O_4)$ unit is found in hexanuclear $[Ln_2(\mu-ox)\{Cr(bpy)(\mu-ox)(ox)\}_4(H_2O)_6]$, $Ln =$

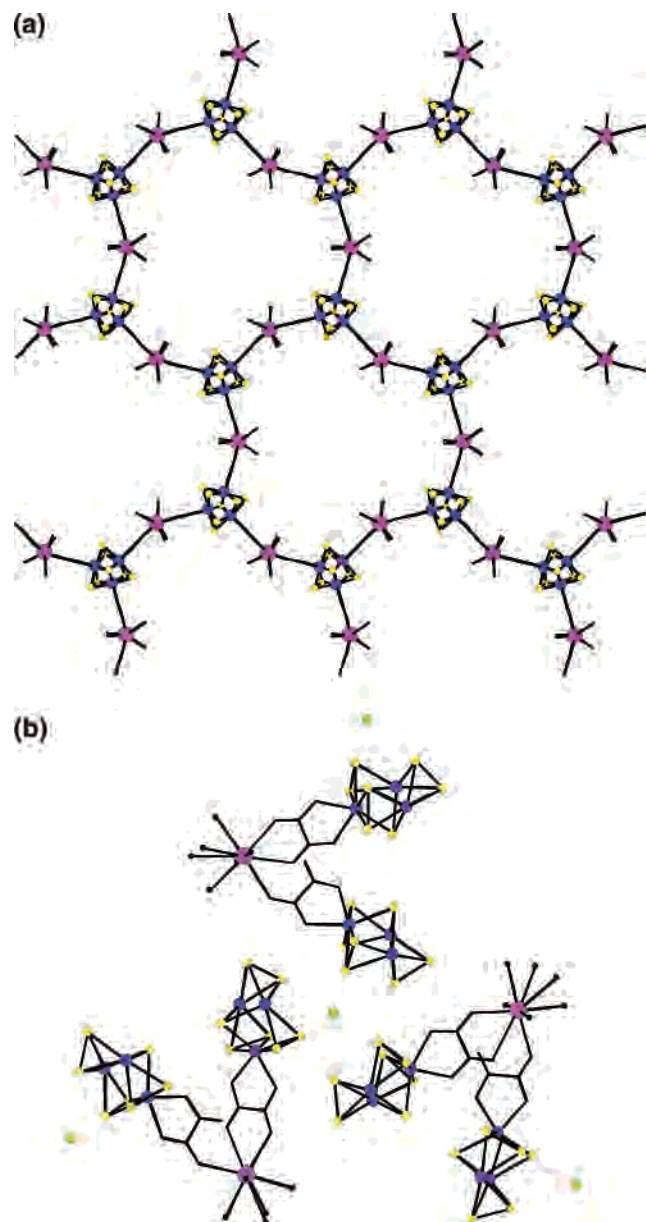


Figure 3. Structure of **I**: (a) the porous cationic layer $\{[\text{Ln}(\text{H}_2\text{O})_6][\text{W}_3\text{S}_7(\text{C}_2\text{O}_4)_3]_n\}^{5n+}$ of fragment **A** and (b) its decoration consisting of three **B** fragments (the layer is not shown for clarity). The second disordered position of the Ln(III) cation and some oxalate groups are not shown here for clarity. The decoration (b) is attached to the layer (a) through $\text{S}_{\text{ax}} \cdots \text{Br}$ contacts.

La,²⁷ Pr.¹¹ In **II**, the molecules are linked into infinite zigzag anionic chains through axial contacts $3\text{S}_{\text{ax}} \cdots \text{Br}^-$ where $d(\text{S}_{\text{ax}} \cdots \text{Br}^-) = 3.02\text{--}3.26 \text{ \AA}$. These bromides are located in the fracture points of the chains (Figure 6). The chains are arranged in a hexagonal motif. The shortening of the Ln–O bonds in the series leads to a regular change in the chain geometry. To describe the latter quantitatively, we introduce stretching parameter α and torsion parameter β (Figure S4). When the Ln–O distances shorten, the cell volume decreases as a whole, but not strictly linearly (Figure S5). The neutral complex molecules that constitute the chain links thus shorten, and the chains straighten, which can be followed

(27) Xing, Z.; Guo-Cong, G.; Fa-Kun, Z.; Guo-Wei, Z.; Jia-Cheng, L.; Hong-Wei, M.; Ming-Sheng, W.; Hui-Yi, Z.; Zheng-Chao, D.; Jin-Shun, H. *Chin. J. Struct. Chem.* **2002**, *21*, 477.

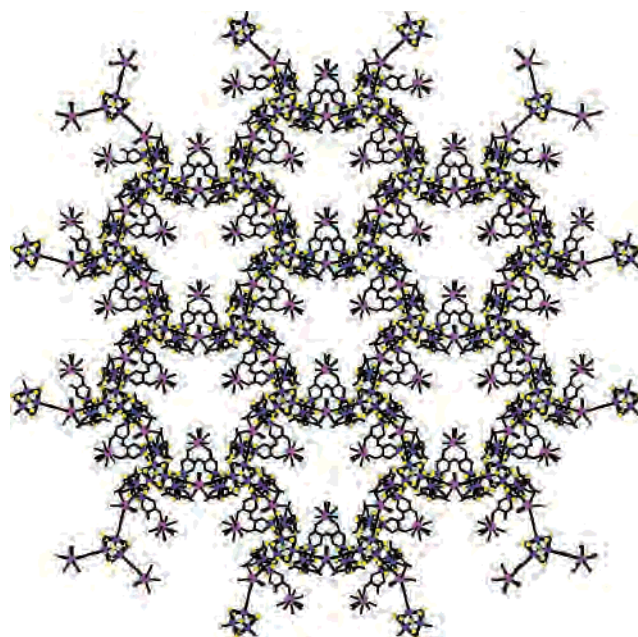


Figure 4. Projection of structure **I** along c_{hex} . The diameter of extended pores is about 9 Å.

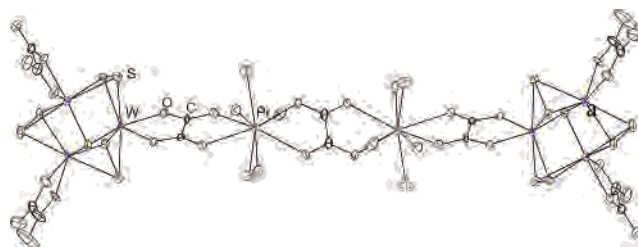


Figure 5. $[(\text{W}_3\text{S}_7(\text{C}_2\text{O}_4)_3\text{Pr}(\text{H}_2\text{O})_5)_2(\text{C}_2\text{O}_4)]$ molecule of **IIa**. Ellipsoids are drawn at the 50% probability level.

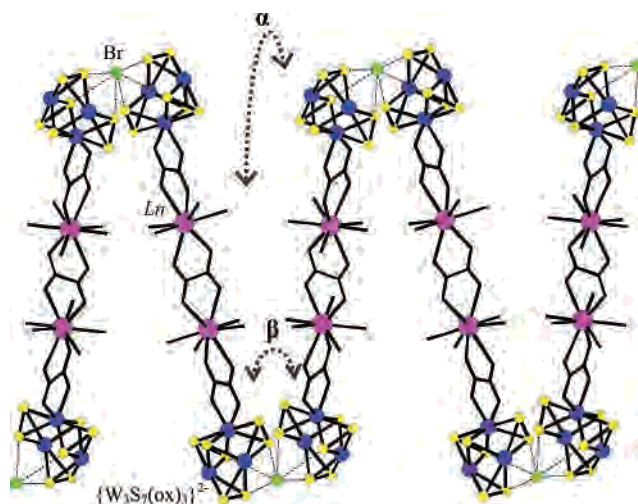


Figure 6. Fragment of polymeric chain $\{[(\text{W}_3\text{S}_7(\text{C}_2\text{O}_4)_3\text{Ln}(\text{H}_2\text{O})_5)_2(\text{C}_2\text{O}_4)\text{Br}]_n\}^{n-}$ in **II** built on axial $3\text{S}_{\text{ax}} \cdots \text{Br}^-$ contacts of $3.02\text{--}3.26 \text{ \AA}$ (dashed lines). The angles α and β characterize the deformation of the chain in two perpendicular directions (shown by double arrows). In the wire presentation, Br, S, W, and Ln atoms are shown, and terminal oxalate ions are not shown.

by increase in the torsion angle β . The evolution of stretching parameter α is not so straightforward, indicating that factors other than the Ln–O bond shortening are also operative (Figure S6).

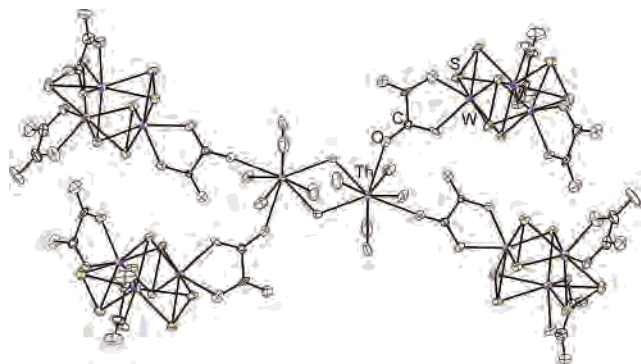


Figure 7. The molecular structure of centrosymmetric anion $[(W_3S_7(C_2O_4)_3)_4Th_2(OH)_2(H_2O)_{10}]^{2-}$ in **III**. Ellipsoids are shown at 50% probability.

Table 3. Th–Th and Th– μ -O Distances for Compounds Containing the $Th_2(\mu-OH)_2^{6+}$ Core

compound	Th–Th (Å)	Th– μ -O (Å)	ref
$K_2[(W_3S_7(C_2O_4)_3)_4Th_2(OH)_2(H_2O)_{10}] \cdot 14.33H_2O$ (III)	3.9641(10)	2.349(9)	this work
$[Th_2(OH)_2(NO_3)_6(H_2O)_6]$	3.988	2.39, 2.33	32
$[Th_2(OH)_2(DAPSC)_2(NO_3)_2(H_2O)_2] \cdot (NO_3)_4 \cdot 4H_2O$, DAPSC = 2,6-diacetylpyridine-disemicarbazone	4.018	2.361, 2.372	33
$[(pic)(H_2O)_6Th(\mu-OH)_2Th(OH)_6(pic)] \cdot (pic)_4 \cdot 20H_2O$, pic = picrate	4.071	2.366, 2.381	34
$[Th_2(OH)_2Cl_2(H_2O)_{12}]Cl_4 \cdot 2H_2O \cdot 18\text{-crown-6}$	3.995	2.362, 2.339	35
$[(Th(OH)_2por)_3]$, por = porphyrin	3.960	2.460, 2.435	36

Notwithstanding directed non-valence $S_{ax} \cdots Br^-$ interactions and expressly nonspherical complex molecules, the packing of these relatively large units $[(W_3S_7(C_2O_4)_3)Ln(H_2O)_5]_2(C_2O_4)$, though very complex, is topologically equivalent to face-centered cubic packing. The K^+ cations and solvent water molecules fill the voids. Interestingly, the α parameter correlates well with the degree of the deviation from the idealized fcc packing. The more a chain is folded, the more distorted the packing becomes (Figure S6).

Compound **III** contains complex anions $[(W_3S_7(C_2O_4)_3)_4Th_2(OH)_2(H_2O)_{10}]^{2-}$ (Figure 7), built around the $\{Th_2(OH)_2\}^{6+}$ dimeric unit, which occupies the inversion center. Each Th atom monodentately coordinates two $[W_3S_7(ox)_3]^{2-}$ ions via oxalate oxygens. The remaining five coordinating sites at Th are occupied with water molecules, $CN(Th) = 9$. The distances in $\{Th_2(OH)_2\}^{6+}$ are in good agreement with other Th bishydroxo complexes (Table 3). The main bond lengths in **III** are given in Table 2. Unlike **I** and **II**, this structure does not contain halides. Instead, the anions $[(W_3S_7(C_2O_4)_3)_4Th_2(OH)_2(H_2O)_{10}]^{2-}$ form dimeric associates between themselves in such a way that the cluster anions $[W_3S_7(ox)_3]^{2-}$ are mutually bound via six $S_{ax} \cdots O$ contacts (Figure 8a) ($S_{ax} \cdots O = 2.927(9)–3.153(9)\text{Å}$) (Table 2). In this way, each anion $[(W_3S_7(C_2O_4)_3)_4Th_2(OH)_2(H_2O)_{10}]^{2-}$ interacts with four other anions, giving rise to layers (Figure 8b). Between the layers, K^+ and disordered solvent water molecules are located. The layers are stacked to allow the center of gravity of $[(W_3S_7(C_2O_4)_3)_4Th_2(OH)_2(H_2O)_{10}]^{2-}$ to build a slightly distorted fcc motif.

Similar aggregation into dimers via carboxylate oxygens occurs in $(Et_3NH)_2[Mo_3S_7(SC_6H_4COO)_3]$.²⁸ There the cen-

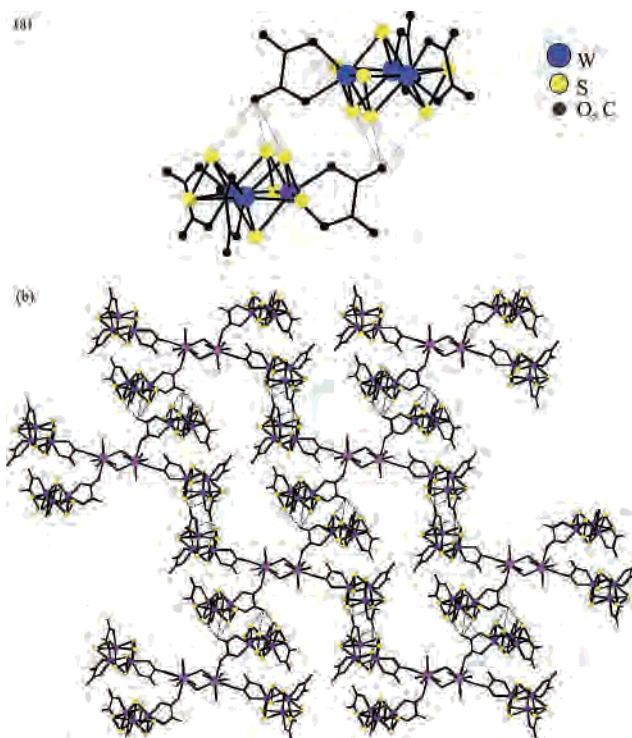


Figure 8. Fragments of the crystal structure in **III**: (a) dimer of two cluster anions $[W_3S_7(ox)_3]^{2-}$ joined by axial $3S_{ax} \cdots O(C_2O_4)^{2-}$ contacts of 2.93–3.15 Å (dashed lines) and (b) the polymeric layer $\{(W_3S_7(C_2O_4)_3)_4Th_2(OH)_2(H_2O)_{10}\}_n^{2-}$ built on the axial contacts. The view is perpendicular to $[112]$ plane (in the wire presentation, S and Th atoms are shown).

trosymmetric associate $\{[Mo_3S_7(SC_6H_4COO)_3]\}_2^{4-}$ is held by shorter (as compared to **III**) contacts $3S_{ax} \cdots O$ (2.709–3.078 Å). The most important difference between this structure and **III** is that in the latter further coordination of the dimeric associates to Th^{4+} creates an infinite polymeric net.

The W–W bonds in the $[W_3S_7(ox)_3]^{2-}$ clusters are somewhat shorter than in $[W_3S_7Br_6]^{2-}$ (2.733–2.744, av 2.736(5) Å, $[W_3S_7Cl_6]^{2-}$ (2.727–2.745 Å), and polymeric $W_3S_7Br_2Br_{4/2}$ (2.699–2.722, av 2.714(13) Å)²⁹ and are close to those observed in $K_{2.5}[W_3S_7(ox)_3]Br_{0.5} \cdot 5H_2O$ (2.697–2.707, av 2.701(6)).⁴ The other distances in **I** and **II** (Table 2) are not exceptional.

Thus, coordination of $[W_3S_7(ox)_3]^{2-}$ to Ln^{3+} or Th^{4+} produces, depending on the cation, either discrete molecular complexes (**I** and **III**) or a layered structure (**II**). The latter type of structure is found in the rare-earth oxalates $Ln_2(C_2O_4)_3 \cdot xH_2O$ ($x = 6–10$; $Ln = Sc, Y, La–Lu$). In that case, the net is built of fused hexagonal $Ln_6(\mu-C_2O_4)_6$ rings, and guest molecules other than water (like N_2H_4) can enter the channels or interlayer space.²¹ The crystal structure of $Gd_2(ox)[Cu(pba)]_3[Cu(H_2O)_5] \cdot 20H_2O$ ($pba = 1,3\text{-propylenebis(oxamate)}$)³⁰ consists of puckered ladderlike strands of $Gd[Cu(pba)]$ units connected into a two-dimensional honeycomb pattern by oxalato groups between two Gd^{3+} ions. Again, distorted hexagonal rings result. Additionally, $[Cu(H_2O)_5]^{2+}$ ions are found between the layers. This shows that layered oxalato-bridged coordination polymers have the

(28) Hegetschweiler, K.; Keller, T.; Baumle, M.; Rihs, G.; Schneider, W. *Inorg. Chem.* **1991**, *30*, 4342.

potential to accommodate various guests. In the structure of $(\text{H}_3\text{O})[\text{Yb}(\text{ox})\text{Ni}(\text{S}_2\text{C}_2\text{O}_2)_2] \cdot 1.5\text{H}_2\text{O}$,³¹ there are cyclic tetramers $(\text{YbO}_2\text{C}_2\text{O}_2)_4$, not hexamers, linking together at Yb into infinite chains by $[\text{Ni}(\text{S}_2\text{C}_2\text{O}_2)_2]^{2-}$.

This work shows that oxalate cluster complex $[\text{W}_3\text{S}_7(\text{ox})_3]^{2-}$ can function as building block for coordination polymers. In fact it participates in building of the polymeric framework in two ways: by direct coordination of a heterometal through oxalate oxygens (serving as node a three-connected net) and

- (29) (a) Fedin, V. P.; Sokolov, M. N.; Gerasko, O. A.; Kolesov, B. A.; Fedorov, V. Ye.; Mironov, A. V.; Yufit, D. S.; Slovohotov Yu, L.; Struchkov, Yu. T. *Inorg. Chim. Acta* **1990**, *175*, 217. (b) Fedin, V. P.; Sokolov, M. N.; Myakishev, K. G.; Gerasko, O. A.; Fedorov, V. Ye.; Maciček, J. *Polyhedron* **1991**, *10*, 1311. (c) Gerasko, O. A.; Virovets, A. V.; Dybtsev, D. N.; Clegg, W.; Fedin, V. P. *Koord. Khim.* **2000**, *26*, 512. (d) Cotton, F. A.; Kibala, P. A.; Matvsz, M.; McCaleb, C. S.; Sandor, R. B. W. *Inorg. Chem.* **1989**, *28*, 2623.
- (30) Guillou, O.; Bergerat, P.; Kahn, O.; Bakalbassis, E.; Boubekeur, K.; Batail, P.; Guillot, M. *Inorg. Chem.* **1992**, *31*, 110.
- (31) Frasse, C.; Trombe, J.-C.; Gleizes, A.; Galy, J. *C. R. Acad. Sci. Paris, Ser. II* **1985**, *300*, 403.
- (32) Johansson, G. *Acta Chem. Scand.* **1968**, *22*, 389.
- (33) Bino, A.; Chayat, R. *Inorg. Chim. Acta* **1987**, *129*, 273.
- (34) Harrowfield, J. M.; Peachey, B. J.; Skelton, B. W.; White, A. H. *Aust. J. Chem.* **1995**, *48*, 1349.
- (35) Rogers, R. D.; Bond, A. H. *Acta Crystallogr.* **1992**, *C48*, 1199.
- (36) Kadish, K. M.; Liu, Y. H.; Anderson, J. E.; Charpin, P.; Chevrier, G.; Lance, M.; Nierlich, M.; Vigner, D.; Dormond, A.; Belkalem, B.; Guillard, R. *J. Am. Chem. Soc.* **1988**, *110*, 6455.

by (axial) contacts, which, in turn, link together the cluster fragments. These structures display attractive possibilities of using non-valence interactions $3\text{S}_{\text{ax}} \cdots \text{Hal}^-$ and $3\text{S}_{\text{ax}} \cdots \text{O}(\text{C}_2\text{O}_4^{2-})$ to diversify crystal packing because they play a significant role in intermolecular interactions.

Acknowledgment. This work is dedicated to Prof. Dr. V. E. Fedorov on the occasion of his 70th birthday. The work was supported by Russian Foundation for Basic Research (Grant 05-03-32126), the Haldor Topsøe Foundation (to A.L.G.) and Presidium of Siberian Branch of Russian Academy of Science (Lavrentiev Grant for Young Scientists to E.V.P.). We thank Professor V. A. Blatov (Samara State University, Russia) for providing the TOPOS 4.0 Professional program suit. M.N.S. is grateful for the Presidential Grant MD 7072.2006.3. Thanks are due to Dr. C. Vincent (University Javme I, Spain) for recording the ESI Mass spectra.

Supporting Information Available: CIF files for structures **Ia**, **Ib**, **IIa–IIc**, and **III** and magnetic susceptibility data for **IIa**, **IIb**, and **IIc**. This material is available free of charge via the Internet at <http://pubs.acs.org>.

IC061540L